Available online at www.sciencedirect.com

SciVerse ScienceDirect

Scripta Materialia 66 (2012) 258–260

Scripta MATERIALIA

www.elsevier.com/locate/scriptamat

Toward the enhancement of thermoelectric properties of lamellar $Ca_3Co_4O_9$ by edge-free spark plasma texturing

Jacques G. Noudem,*[,1] Driss Kenfaui, Daniel Chateigner and Moussa Gomina

CRISMAT, UMR 6508 ENSICAEN/CNRS, IUT-Caen, Université de Caen Basse-Normandie, 6 Bd Maréchal Juin, 14050 Caen Cedex 04, France

Received 24 July 2011; revised 3 November 2011; accepted 4 November 2011
Available online 11 November 2011

A spark plasma sintering (SPS) device was modified to allow free deformation of grains perpendicular to the loading axis. The aim was to obtain lamellar thermoelectric $Ca_3Co_4O_9$ ceramics. The new process is referred to as edge-free spark plasma sintering or spark plasma texturing (SPT). SPT materials are compared to those processed by conventional sintering and traditional SPS in terms of microstructure, texture and high-temperature thermoelectric properties. The results highlight the decisive advantages of the SPT technique.

Keywords: Edge-free spark plasma sintering (ESPS); Spark plasma texturing (SPT); Texturation; Grain growth; Grain boundaries density

Spark plasma sintering (SPS) is a relatively new technique [1–4] that has been developed for shaping materials by combining simultaneously uniaxial loading (using direct contact with the sample) and the application of an electric field, of up to 250 kN and 10 kA, respectively. Even though the key mechanisms controlling SPS are still debated (the Joule effect and/or plasma generation due to the spark), this method shows a number of advantages [1,4] – (i) an increase in the kinetics of sintering, (ii) rapid densification and (iii) grain growth limitation – which are helpful for tailoring the microstructure of functional materials and thus optimize their transport, mechanical and/or thermal properties.

A lack of homogeneity has been reported in the microstructure of materials processed by SPS [1,4]: the core of the samples exhibits higher densities than the outer regions. Indeed, microcracks and larger pores are present in these outer regions. If the presence of microcracks can be explained by the shear stress exerted by the wall of the mould on the sample during SPS processing, as creep is the major deformation mechanism, the level of this stress (and thus the size of the homogeneous core) depends on the elaboration conditions in a more or less uncontrolled manner. These defects might explain the discrepancies observed among the results reported in the literature. To avoid (or minimize) these defects, we propose the use of a mould with a diameter much larger than the desired final diameter of the sintered sample. Under such circumstances, the sample behaves like in an edge-free mould (the hot-pressing configuration). This large-diameter configuration is referred to as edge-free spark plasma sintering or spark plasma texturing (SPT) (Fig. 1). The results presented in this letter are for samples prepared by the conventional sintering (CS) route and the SPS and novel SPT methods.

The elaboration of the samples using the SPT process was conducted similarly to the SPS: identical equipment and the same loading and heating profiles were used [3,5,6]. Basically, in the SPT method, the starting powder was first sintered at 900 °C for 2 h in a mould with a diameter of 13 mm in order to obtain a self-supporting sample. This $Ca_3Co_4O_9$ (Co349) preform was ten placed in the centre of a graphite mould with a diameter of 20 mm, as shown in Figure 1b. SPT is accompanied by a remarkable change in the grains' morphology, progressively transforming them into platelets. The idea is to induce free deformation of the pellet. During this stage, the lamellar platelets are growing and aligned with their *c*-axis parallel to the applied uniaxial force. For the reference sample, the Co349 powder was introduced directly into the mould, in the same way as in traditional SPS sintering (Fig. 1a).

* Corresponding author. Tel.: +33 231 451 366; fax: +33 231 451 309; e-mail: jacques.noudem@ensicaen.fr

[1] Present address: LUSAC, UCBN, rue Aragon, 50130 Cherbourg, France.

1359-6462/$ - see front matter © 2011 Acta Materialia Inc. Published by Elsevier Ltd. All rights reserved.
doi:10.1016/j.scriptamat.2011.11.004

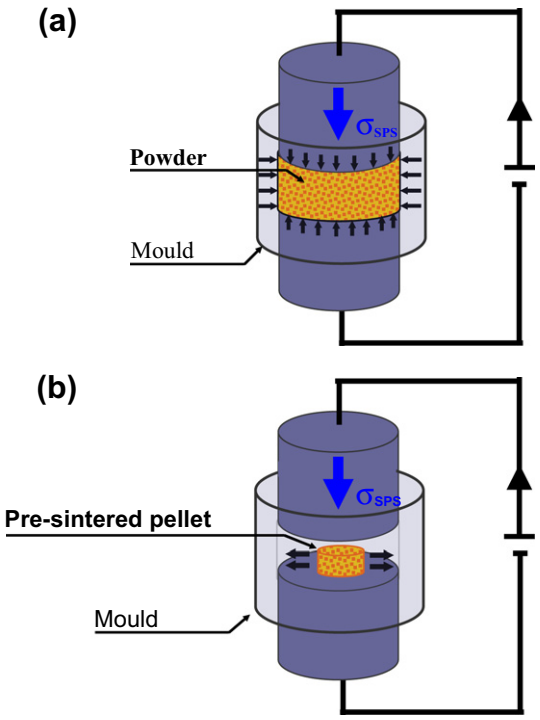

Figure 1. Schematic configuration of the SPS and SPT processes.

Quantitative texture analyses were operated using a 4-circle X-ray diffractometer equipped with a curved position sensitive detector (CPS120 from INEL), simultaneously spanning 100° in 2θ [7]. We measured 864 2θ diagrams for as many sample orientations in the Eulerian cradle, in a 0–55° tilt angle range (in 5° steps) and a 0–355 azimuthal angle range (in 5° steps). The orientation distribution of crystallites was determined using the whole diffraction pattern analysis in a combined Rietveld–EWIMV formalism [8–10], implemented using the MAUD software [11]. During these steps, we refined the unit-cell parameters of Co349. The results are compared with materials obtained by CS and SPS. Thermoelectric properties and performance factors were measured using ULVAC-RIKO (ZEM3 model, Yokohama, Japan). The temperature dependence of electrical resistivity, ρ, and Seebeck coefficient, S, measurements were simultaneously performed on ~10 mm × 2 mm bar-shaped specimens cut from the samples in a direction perpendicular to the pressing axis. When a temperature gradient is applied between the ends of a specimen, the induced voltage was measured and the Seebeck coefficient was obtained as: $S = \Delta V/\Delta T$.

The ρ measurement is based on the four-probe method, using an applied electric current. The resistance, R, of the specimen is calculated from the resulting voltage V and the applied current I as: $R = V/I$. The electric resistivity, ρ, is then determined as follows: $\rho = R \times (A/L)$, where A is the specimen section area and L is the distance between the two measurement points.

Figure 2 shows the microstructure of the samples processed by the CS, SPS and SPT methods. While almost round shape grains are obtained by CS (Fig. 2a), close-packed platelets are obtained when implementing SPS (Fig. 2b), indicative of increased crystal growth. However, the arrangement of these platelet aggregates exhibits no preferred orientation. On the other hand, the aggregates are pronouncedly oriented with their plane perpendicular to the loading direction (vertical direction of Fig. 2c) when produced by SPT. The size of the Co349 lamellar grains reaches 9 and 14 μm for the SPS and SPT processed samples, respectively. A similar experimental procedure was used by Gopalan et al. [12] to induce grain alignment by hot-pressing Nd–Fe–B permanent magnet powder. Comparison of Figure 2b and c demonstrates the detrimental influence of the mould wall on the microstructure of these materials. In fact, the microstructure of the SPT sample is similar to the one usually obtained with the hot-pressing process (HP) [13,14]. The decisive benefit of SPT over HP is the short sintering time and subsequently the energy saving (45 min for SPT compared to 36 h for HP).

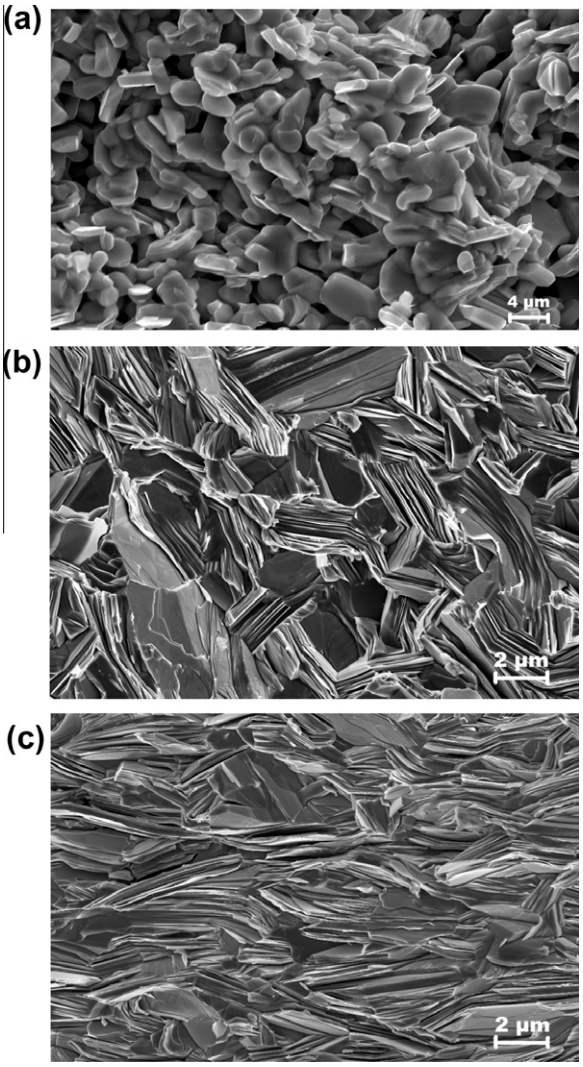

Figure 2. Typical microstructures obtained from (a) CS, (b) SPS and (c) SPT.

Moreover, the relative density obtained is ~98% for both SPS and SPT samples, while it is only 60% for the CS sample. A homogeneous microstructure was obtained across all the SPS and SPT samples, but a key difference between them is that in the latter process

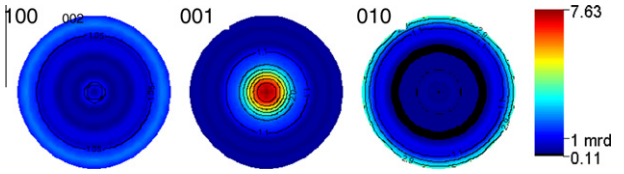

Figure 3. {100}, {002} and {010} pole figures of the Co349 SPT sample. The refinement was obtained within the $P2_1/m$ supercell space group and resulted in cell parameters of $a = 4.851(1)$ Å, $b = 36.108(2)$ Å, $c = 10.7852(8)$ Å and $\beta = 98.20(1)$. Reliability factors for the orientation distribution function were $R_w = 2.2\%$ and $R_B = 2.4\%$, with a goodness of fit of 1.37 for the Rietveld fits of all the diagrams.

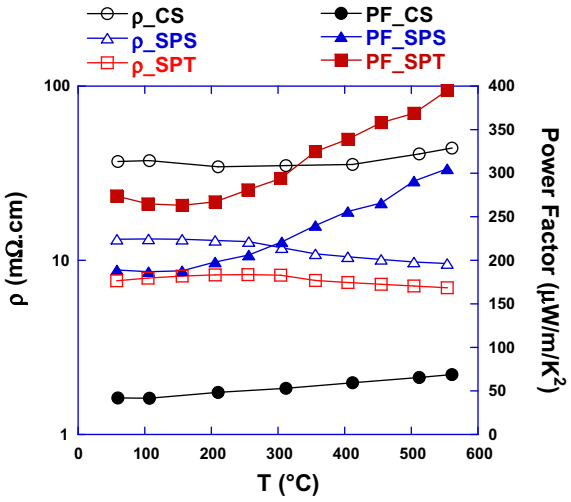

Figure 4. Temperature-dependent electrical resistivity and power factor curves of the CS, SPS and SPT samples.

needs a loosely consolidated sample (as the grains are no longer confined by the mould wall).

The crystallographic texture of the SPT sample is indicated by a maximum of 7.6 multiples of random distribution (mrd) on the {001} pole figure (Fig. 3) with no significant preferred orientation around the load axis (see the {100} and {010} pole figures). The imposed texture still remains fibre-like, but the maximum of the reciprocal c-axis orientation density is approximately doubled under optimized conditions compared to the SPS elaboration [5–14]. The global texture strength corresponds to a texture index of $F^2 = 12.2$ mrd^2, the largest obtained using the SPS method.

The temperature dependence of the resistivity of the SPS and SPT samples is shown in Figure 4. The lowest values are noted for the SPT sample, which correlates well with the microstructure features presented in Figure 2c: (i) plate-like morphology of the grains; (ii) a reduction in grain boundary densities in the plane perpendicularly to the loading direction; and (iii) sample densification and a stronger texture. At 550 °C, the in-plane electrical resistivity of the CS, SPS and SPT samples are ~44, 10 and 7 mΩ cm, respectively. The evolution of the resistivity vs. temperature shows a transition around $T^* =$ 250 °C, which has been attributed to a magnetic [15] or structural transition [16]. Beyond T^*, the SPS and SPT samples exhibit a semi-conducting behaviour, while the CS sample shows a metallic behaviour, probably due to the higher resistivity component along the c-axis. The Seebeck coefficient values, S, are close to each other for all samples as this parameter is principally influenced by the chemical composition, whereas the electrical resistivity strongly depends on their microstructure. The power factor (PF), expressed by S^2/ρ, is an important parameter that allows an evaluation of the thermoelectric performances of a given material. The PF values increase monotonously with temperature for both the SPS and SPT samples (Fig. 4). At 550 °C, a maximum PF value of 400 μW m^{-1} K^{-2} is reached for the SPT sample, which is almost 30% higher than the corresponding value for SPS [5] and eight times larger than that for the CS samples [5].

We conclude from this investigation that the newly developed SPT technique offers a new way to process lamellar systems like $Ca_3Co_4O_9$, in order to improve their anisotropic properties like transport currents and Seebeck-related coefficients. There is a priori no main drawback attached to this technique, which could be used for the anisotropic elaboration of other compounds.

[1] M. Tokita, Mater. Sci. Forum 492–493 (2005) 711.
[2] C. Elissalde, M. Maglione, C. Estournès, J. Am. Ceram. Soc. 90 (2007) 973.
[3] Y. Liu, Y. Lin, Z. Shi, Ce-W. Nan, Z. Shen, J. Am. Ceram. Soc. 88 (2005) 1337.
[4] R. Orru, R. Licheri, A.M. Locci, Al. Cincotti, G. Cao, Mater. Sci. Eng., R 63 (2009) 127.
[5] D. Kenfaui, G. Bonnefont, D. Chateigner, G. Fantozzi, M. Gomina, J.G. Noudem, Mater. Res. Bull. 45 (2010) 1240.
[6] J.G. Noudem, M. Prevel, A. Veres, D. Chateigner, J. Galy, J. Electroceram. 22 (2009) 91.
[7] M. Morales, D. Chateigner, L. Lutterotti, J. Ricote, Mater. Sci. Forum 408 (2002) 113.
[8] D. Chateigner, Combined Analysis, ISTE-Wiley, London, 2010, p. 496.
[9] H.M. Rietveld, J. Appl. Crystallogr. 2 (1969) 65.
[10] L. Lutterotti, D. Chateigner, S. Ferrari, J. Ricote, Thin Solid Films 450 (2004) 34.
[11] L. Lutterotti, S. Matthies, H.-R. Wenk, in: J.A. Szpunar (Ed.), Textures of Materials: Proceedings of ICOTOM12, National Research Council of Canada, Ottawa, 1999, pp. 1599–1604.
[12] R. Gopalan, H. Sepehri-Amin, K. Suresh, T. Ohkubo, K. Hono, T. Nishiuchi, N. Nozawa, S. Hirosawa, Scripta Mater. 61 (2009) 978.
[13] M. Prevel, S. Lemonnier, Y. Klein, S. Hébert, D. Chateigner, B. Ouladdiaf, J.G. Noudem, J. Appl. Phys. 98 (2005) 093706.
[14] D. Kenfaui, D. Chateigner, M. Gomina, J.G. Noudem, Int. J. Appl. Ceram. Technol. 8 (2011) 214.
[15] A.C. Masset, C. Michel, A. Maignan, M. Hervieu, O. Toulemonde, F. Studer, B. Raveau, J. Hejtmanek, Phys. Rev. B62 (2000) 166.
[16] H. Muguerra, D. Grebille, Acta Crystallogr., Sect. B 64 (2008) 676.